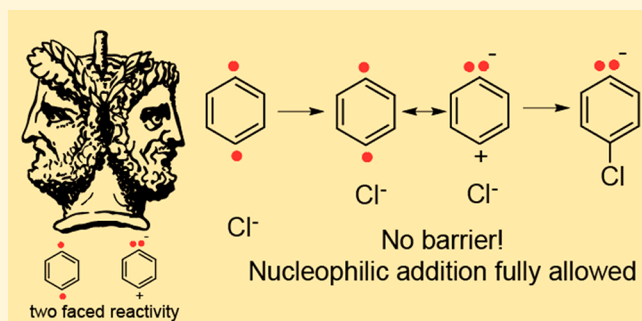


Nucleophilic Addition to Singlet Diradicals: Homosymmetric Diradicals

Paul G. Wentholt*[†] and Arthur H. Winter*[‡][†]The Department of Chemistry and Biochemistry, Purdue University, West Lafayette, Indiana 47906, United States[‡]The Department of Chemistry and Biochemistry, Iowa State University, Ames, Iowa 52101, United States

Supporting Information

ABSTRACT: Experiments have demonstrated that nucleophiles can attack singlet diradicals to generate bonded, closed-shell addition products. Here, we present a molecular orbital analysis for this reaction, focusing on the addition of nucleophiles to homosymmetric diradicals. We show that beginning with the Salem–Rowland molecular orbital description of homosymmetric diradicals, a continuous progression from open-shell diradical to closed-shell addition product occurs during the reaction via a gradual evolution of orbital and configuration interaction coefficients. This theoretical framework is supported by high-level multi-reference computations (CASPT2, EOM-SF-CCSD(dT)) using the addition of chloride to *p*-benzyne to generate a *p*-chlorophenyl anion as a case study. When using levels of theory that include dynamic correlation, the reaction is predicted to be barrierless. No abrupt switch from diradical to closed-shell species happens during the mechanism, but rather a gradual decrease in diradical character occurs as the nucleophile approaches the radical center before ultimately transforming into the closed-shell anion. The overarching conclusion from this work is that there are no electronic impediments of any kind, deriving from orbital symmetry or from any other source, that exist for the addition of nucleophiles to homosymmetric singlet diradicals.



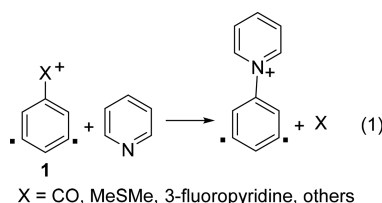
INTRODUCTION

The addition of nucleophiles to electrophiles is a fundamental concept in the understanding of chemical reactions. It is also readily understood even through a model as simple as Lewis theory, where the electrophile accepts a pair of electrons from the nucleophile to create a shared pair (bond). Although more detailed treatments can be considered,¹ the basics of the reaction remain the same, with a two-electron interaction to create a bonding orbital.²

Nucleophilic addition is more complicated when it involves more than addition of an electron pair to an empty orbital. For example, nucleophilic addition to a phenyl radical is possible with sufficiently strong nucleophiles,^{3–6} but the predominant reaction expected for radicals is radical addition or radical abstraction. Nucleophilic addition requires a single-electron transition from the σ to π orbital, which is formally symmetry forbidden for the planar system. Therefore, describing the pathway for nucleophilic addition to radicals (the $S_{RN}1$ mechanism) requires consideration of the orbitals involved^{7–12} and the different electronic states possible.^{13,14}

Similarly, diradicals are generally expected to react via radical abstraction, due to their open-shell nature. Indeed, this is generally the case, as hydrogen atom and other radical abstractions are commonly observed.^{15–21} However, in select cases, diradicals have been found to undergo nucleophilic addition. For example, by using mass spectrometry, Kenttämäa

and co-workers^{22,23} examined the reactivity of ionized derivatives of *m*-benzyne (**1**) and found them to undergo substitution reactions with pyridine substrates (eq 1). Similarly,

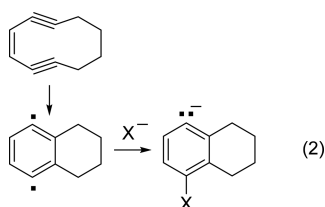


Perrin and co-workers²⁴ found that nucleophilic addition occurs with *p*-benzyne derivatives formed by a Bergman cyclization (eq 2). Although *p*-benzyne is a ground-state singlet, the coupling between the electrons is small ($\Delta E_{ST} = 2–4$ kcal/mol),²⁵ and radical reactivity is commonly observed.^{26,27} As with nucleophilic addition to radicals, there are no simple “arrow pushing” mechanisms that can be drawn for the addition to diradicals, although they can be shown by using a combination of double-headed and single-headed arrows.²⁸

Whereas arrows can provide a notation of how the bonding changes upon addition of a nucleophile to the diradicals, it does

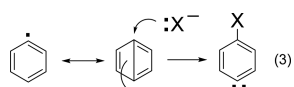
Received: June 5, 2018

Published: September 10, 2018



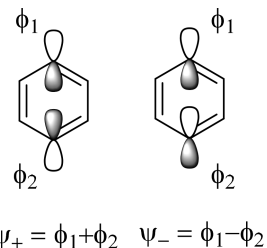
not provide an explanation for how or why it occurs. For *m*-benzyne, Kenttämäa and co-workers²³ considered a curve crossing model to balance the effects of (favorable) bond formation and (nonfavorable) formal charge separation. In this model, there is a barrier for the addition of the neutral nucleophile that results from creation of charge separation, but there is no indication that there is a symmetry barrier for the reaction. In fact, addition of chloride to *m*-benzyne to form the 3-chlorophenyl anion (and thus not creating charge separation) was calculated by using the (restricted) BLYP approach to occur without an energy barrier.

To account for the addition of nucleophiles to *p*-benzyne, Perrin and Reyes-Rodriguez²⁸ described the reaction in terms of a bicyclic (Dewar) benzene structure, with the second carbon acting as a “leaving group” (eq 3). From an orbital perspective,



the doubly occupied molecular orbital in the bicyclic system is the antisymmetric combination of the atomic orbitals, Ψ_- , which is lower in energy than Ψ_+ due to through-bond coupling (Scheme 1).²⁹ A similar approach could be used to describe the addition of a nucleophile to cyclic *m*-benzyne, wherein the bonding orbital is the doubly occupied, Ψ_+^2 configuration.

Scheme 1



Calculations that allow for open-shell character show that nucleophilic addition to *p*-benzyne occurs without barrier in the gas phase,²⁸ consistent with the reaction occurring without symmetry or orbital constraints, as would be the case in eq 1.

Although conceptually straightforward, it is not clear how applicable this approach is, in general. In particular, the single electronic configurations, Ψ_+^2 and Ψ_-^2 , are generally not accurate representations of the wave function for diradical systems. As described by Salem and Rowland,³⁰ although the Ψ_+^2 and Ψ_-^2 configurations work well for bonding systems where there is extensive overlap of the atomic orbitals, they contain too much polar character to properly describe systems like diradicals where the overlap between the atomic orbitals is small. In a diradical such as *m*-benzyne, where there can be extensive overlap of the back-sides of the nonbonding atomic orbitals, especially at the bicyclic geometry,^{31–33} a closed-shell configuration or restricted density functional theory calculation

may provide a reasonable approximation of the actual electronic structure,^{34,35} but that does not apply for a diradical such as *p*-benzyne, where the overlap of the orbitals is predominantly through-bond²⁹ and not through-space.

Alabugin and co-workers have provided an alternate perspective, recognizing that there is weak electron coupling, even in systems like *p*-benzyne that are nominally diradical.³⁶ The consequence of this coupling is that it results in energy stabilization that must be overcome in a free radical process,^{37,38} but not during nucleophilic addition. Alternatively, breaking the symmetry through substitution can polarize the system, and the additional zwitterionic character allows for nucleophilic addition.^{36,39,40} However, nucleophilic addition also occurs with symmetric diradicals, which do not, in themselves, have polarized electronic structures.²⁴

In this work, we provide a more detailed examination of the mechanism for nucleophilic addition to homosymmetric diradicals, such as *p*-benzyne, from a molecular orbital perspective. We are able to show that, when using an appropriate multiconfigurational wave function approach, there are no electronic structure impediments expected for the addition of nucleophiles to these diradicals. This is confirmed by high level, multireference electronic structure calculations, which show that the addition occurs without an activation barrier and that the transition from a diradical reactant to a closed-shell product occurs continuously.

Bond Dissociation as the Reverse of Nucleophilic Addition. Perhaps the biggest challenge in the investigation of nucleophilic addition to diradicals is the initial generation of the diradical. Previous studies have been limited to diradicals generated by cyclization,²⁴ or in the gas phase,^{22,23} such that there is not an easy approach for the general study of the reaction. However, it should be noted that the same considerations that apply to the addition of nucleophiles to diradicals can be applied to the reverse process, such as the elimination of the nucleofuge from an anionic precursor. For example, Wentholt and Squires used collision-induced dissociation to generate aromatic diradicals via α,n eliminations of halogen-substituted anions.^{41–43} Successful thermochemical measurements in these experiments are predicated on having the dissociation occur without an activation barrier in excess of the exothermicity. If this is the case, as was argued, then it requires that the reverse reaction, nucleophilic addition to the diradical, occurs without an activation barrier. Therefore, the fact that diradicals can be formed by elimination indicates that nucleophilic addition to the diradical can occur. So how does that happen?

Theoretical Development. We use the Salem and Rowland description of diradicals as the framework for this discussion.³⁰ From this perspective, diradicals such as the benzenes are “homosymmetric diradicals”, where the nonbonding atomic orbitals can mix by symmetry. Therefore, nonbonding molecular orbitals for *m*- and *p*-benzyne are the symmetry-adapted combinations, $\Psi_+ = \phi_1 + \phi_2$ and $\Psi_- = \phi_1 - \phi_2$, as shown in Scheme 1,⁴⁴ leading to the two-configuration wave function, as in eq 4.

$$\lambda \Psi_+^2 - \sqrt{1 - \lambda^2} \Psi_-^2 \quad (4)$$

In the homosymmetric diradicals, the size of λ reflects the extent of bonding between the two centers, ranging from $2^{-1/2}$ for pure diradical, which is close to the situation for *p*-benzyne, to

approaching 1 when there is more extensive bonding, as in *m*-benzyne.³⁵

In order to consider the process of nucleophilic addition to the diradical, we describe the wave function of the adduct by using the same type of multiconfiguration wave function. Our approach is to view the nucleophile as a perturbation on the molecular orbital. As the nucleophile approaches, it breaks the degeneracy of the atomic orbitals, ϕ_1 and ϕ_2 , such that it changes the coefficients in the linear combination of atomic orbitals (LCAO), as in eq 5, where $n_1^2 + n_2^2 = 1$.

$$\psi_+ = n_1\phi_1 + n_2\phi_2 \quad (5a)$$

$$\psi_- = n_2\phi_1 - n_1\phi_2 \quad (5b)$$

From a structural perspective, the second effect of adding a nucleophile is that it eliminates the symmetry element that relates ϕ_1 and ϕ_2 in the free diradical. Therefore, the wave function for the homosymmetric diradical (eq 4) is no longer appropriate because $c_1 \neq c_2$, and we need to treat it as a *nonsymmetric* system, where the wave function involves three configurations (eq 6).

$$\Psi = c_1\phi_1^2 + c_2\phi_2^2 + c_{12}\phi_1\phi_2 \quad (6)$$

The wave function for the diradical in the presence of the nucleophile will have optimized values of n_1 and n_2 , the LCAO coefficients, and c_1 , c_2 , and c_{12} , the configuration interaction (CI) coefficients.

The transition from a diradical to a closed-shell system is summarized in Figure 1. Nonpolarized homosymmetric

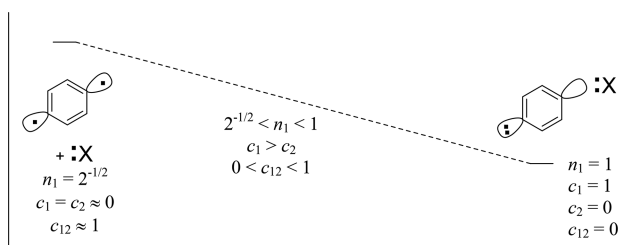


Figure 1. Changes in the coefficients in the orbitals (eq 5) and wave function (eq 6) during nucleophilic addition to *p*-benzyne.

diradicals, such as the benzyne, are described by using $n_1 = n_2$ and λ (eq 4), such that $c_1 = c_2$ and c_{12} depends on the value of λ . Polarized, zwitterionic character in the diradical is introduced by varying the coefficients n_1 and n_2 and by changing the relative contributions of the closed-shell (ϕ_1^2 and ϕ_2^2) and open-shell ($\phi_1\phi_2$) configurations. In the limit where the nucleophile has added to the diradical (the phenyl anion), $n_1 \approx 1$ and the wave function reduces to essentially ψ_+^2 (ϕ_1^2), with no contribution from $\phi_1\phi_2$ or ϕ_2^2 .

The most important conclusion of this analysis is that, because there is no qualitative change in the form of the wave function, and it is merely an issue of varying coefficients, the addition of the nucleophile can occur with a continuous evolution from diradical to the adduct or, in dissociation, from adduct to diradical.

COMPUTATIONAL METHODS

The addition of chloride as a nucleophile to diradicals (conversely, the elimination of chloride from the corresponding anion to form the diradical) has been investigated by using state-averaged multiconfiguration self-consistent field (SA-CASSCF), equation-of-motion

spin-flip coupled-cluster (EOM-SF-CC), and unrestricted B3LYP calculations. The relaxed potential energy surface for the addition was calculated as a function of carbon–chlorine distance.

SA-CASSCF. In order to describe the transition from anion to diradical correctly, SA-CASSCF theory was used. Unlike standard CASSCF calculations, which only include the closed-shell configurations (ψ_+^2 and ψ_-^2), the SA-CASSCF calculation mixes in the excited A_1 state, with a $\psi_+\psi_-$ configuration, which is necessary to obtain the proper wave function at intermediate distances. In terms of atomic orbitals, the $\psi_+\psi_-$ configuration in *p*-benzyne is the zwitterionic state, $\phi_1^2 - \phi_2^2$. In the intermediate geometries, it is going to be more complicated, having the form $n_1^2\phi_1^2 - n_2^2\phi_2^2$, reflecting the unequal contributions of n_1 and n_2 . The active space chosen for the dissociation of *p*-chlorophenyl anion included all the π electrons and π^* orbitals, the σ orbital containing the anion lone pair, and the C–Cl σ and σ^* electrons and orbitals. An additional four a_1 orbitals were added to the active space representing additional C–C σ electrons and orbitals to give a total active space of 16 electrons in 14 orbitals (resulting in 7 a_1 , 2 a_2 , and 5 b_1 irreducible representations).

A relaxed scan of the C–Cl coordinate of the *p*-chlorophenyl anion was conducted using a CASPT2//SA-CASSCF procedure. Specifically, a relaxed PES scan of the C–Cl coordinate was conducted for the 1A_1 state of the *p*-chlorophenyl anion under C_{2v} symmetry at the SA-CASSCF(16,14)/aug-cc-pVTZ level using the MOLCAS 8.2 software package.⁴⁵ Due to a near-degeneracy of the two 1A_1 states along the C–Cl coordinate at long C–Cl distances, state averaging was employed, giving a 1:1 weighting to the two lowest roots. CASPT2(16,14)/aug-cc-pVTZ single points were conducted at the SA-CASSCF geometries to capture dynamical correlation.

A more rigorous treatment of the multiconfigurational character of the system in the transition region could be obtained by using a multistate (MS) CASPT2 calculation.⁴⁶ However, the most important use of MS-CASPT2 is to compensate for deficiencies in the active space; given the extensive size of the active space used in this work, there is less of a need to use the MS-CASPT2 approach. Moreover, considering that this work is not focused on accurate absolute energies, consistency in the methods should be sufficient to draw conclusions regarding the energies.

EOM-SF-CCSD. We have also examined the loss of chloride from *p*-chlorophenyl anion by using the EOM-SF-CC approach, wherein the singlet state is calculated by using a high-spin (triplet) reference with a spin-flipping operator. The SF approach is capable of calculating systems with multiconfigurational character and can include all necessary configurations.

Geometry optimizations were carried out at the EOM-SF-CCSD/6-31+G* level of theory, which include single and double excitations, using unrestricted Hartree–Fock (UHF) orbitals as the reference orbitals. Although spin-contamination in the UHF wave function of the reference state can have an effect on the computed energies of the spin-flip states, the effect on the optimized geometries should be minimal. Fortunately, spin-contamination was not a significant problem in the geometry optimizations, as the $\langle S^2 \rangle$ values for the reference states were all less than 2.1. Single-point energies were calculated at the EOM-SF-CCSD(dT)/6-31+G* level of theory, which includes perturbative treatment of triple excitations, using UB3LYP orbitals as reference orbitals. Whereas a small basis set was used in these calculations for reasons of computational cost, the effect of the basis set is likely largest on the absolute values of the relative energies and less on the shape of the potential energy surface, which is more strongly dependent on the level of correlation than on the basis set.

UB3LYP. Finally, the potential energy surfaces were also calculated by using an unrestricted singlet calculation, at the B3LYP/6-31+G* level of theory. The resulting wave functions for these calculations are mixed singlet and triplet states, as characterized by the expectation value for the $\langle S^2 \rangle$ operator. For a “half-and-half” state, which would be a pure diradical, $\langle S^2 \rangle = 1.0$. Increasing amounts of closed-shell character in the wave function decrease the value of $\langle S^2 \rangle$, which naturally = 0 for a purely closed-shell singlet state. Energies in this work are the raw UB3LYP singlet energies and are not corrected for spin-contamination.

Electronic Structure Analyses. Each of the computational methods described above includes approaches for wave function analysis that allow us to examine the transition from the closed-shell anion to the diradical. For the CASPT2 calculations, we utilize the relative weights of the closed-shell and open-shell configurations in the lowest energy root of the multiconfigurational wave function. This approach most closely resembles the analysis described in the **Theoretical Development** section. Because the orbitals n_1 and n_2 remain essentially localized in the presence of chlorine at the distances examined in this work, the three most important configurations are the closed-shell configurations, effectively ϕ_1^2 and ϕ_2^2 and the diradical configuration, $\phi_1^1\phi_2^1$. At short distances, the wave function would be expected to be essentially ϕ_1^2 , with $\phi_1^1\phi_2^1$ being dominant at longer distances. Therefore, the transition from closed-shell to diradical can be monitored by considering the relative weights of these two configurations. We calculated the fraction of diradical character in the overall wave function, by using the expression in [eq 7](#), where $c_{\phi_1^2}$ and $c_{\phi_2^2}$ are the coefficients for all the phenyl anion configurations, and $c_{\phi_1\phi_2}$ are the coefficients for the benzyne diradical configurations.

$$\frac{\sum c_{\phi_1\phi_2}^2}{\sum c_{\phi_1^2}^2 + \sum c_{\phi_2^2}^2 + \sum c_{\phi_1\phi_2}^2} \quad (7)$$

To assess the transition from closed-shell to diradical in the SF-CCSD calculations, we use the Head-Gordon index, which is computed from state density matrices. In this work, we use the nonlinear variant ([eq 8](#)):^{47,48}

$$N_{u,\text{nl}} = \sum_{i=1}^M n_i^2 (2 - n_i)^2 \quad (8)$$

where M is the total number of orbitals and n_i is the occupation number for each natural orbital. The value of $N_{u,\text{nl}}$ is a measure of the effective number of unpaired electrons, such that for a closed-shell system it is 0, a radical gives 1, and a perfect diradical gives 2, etc. Previous studies have found that the value of $N_{u,\text{nl}}$ for *p*-benzyne, calculated with a cc-pVTZ basis set, is 1.45,³⁴ consistent with the expectation that *p*-benzyne is mostly diradical but has some closed-shell character due to nonperfect degeneracy of the nonbonding orbitals. The Head-Gordon parameter considers populations within natural orbitals and therefore does not depend on the choice of molecular orbitals. Similarly, natural orbital populations are available from the SA-CASSCF calculations, which could be used to examine the changes in the wave function during dissociation. Diradical character in the UB3LYP calculations is monitored by using $\langle S^2 \rangle$ values.

Nucleophilic Addition to *p*-Benzene. Perrin and Reyes-Rodriguez have examined the addition of chloride to *p*-benzyne by using unrestricted BPW91 calculations and have shown that the approach of the chloride occurs without a barrier. This is consistent with the analysis in the preceding section, which predicts there should not be any symmetry restrictions to the reaction. In this work, we re-examine the dissociation in the context of the multireference framework provided above. Therefore, we have carried out multiconfigurational (CASSCF and EOM-SF-CCSD) calculations of the *p*-chlorophenyl anion and its dissociation into *p*-benzyne and chloride, in order to monitor the changes that occur in the wave function.

[Figure 2](#) shows the relative energies for dissociation of *p*-chlorophenyl anion to chloride and *p*-benzyne, calculated at the CASPT2(16,14)/aug-cc-pVTZ, EOM-SF-CCSD(dT)/6-31+G*, and UB3LYP/6-31+G* levels of theory. At all three levels of theory, the addition of chloride to *p*-benzyne occurs without an electronic energy barrier. The absolute energy differences between the *p*-chlorophenyl anion minimum and the structure at a large C–Cl distance range from about 34 kcal/mol (UB3LYP) to 39 kcal/mol (EOM-SF-CCSD(dT)). Considering that these energies refer to geometries still containing Cl^- restricted to C_{2v} geometries and do not refer to complete dissociation with relaxation, they are in reasonable agreement with the experimental value of 35.3 ± 2.0 kcal/mol.⁴¹ More important than the quantitative

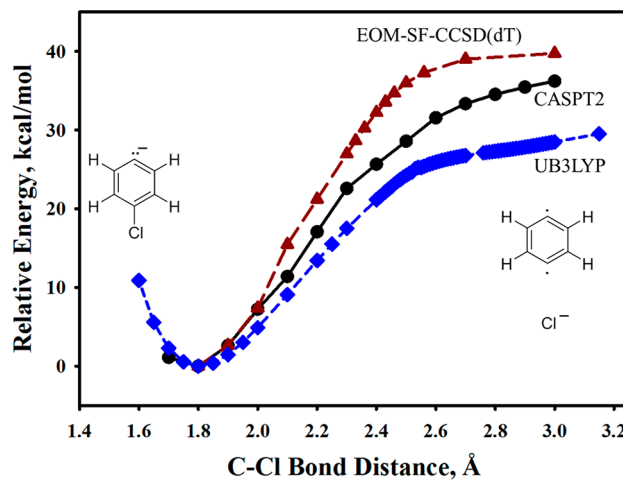


Figure 2. Relative energies for the dissociation of *p*-chlorophenyl anion, calculated at the CASPT2(16,14)/aug-cc-pVTZ (black circles), EOM-SF-CCSD(dT)/6-31+G* (red triangles), and UB3LYP/6-31+G* (blue diamonds) levels of theory.

agreement, however, is the shape of the curve, which shows no activation barrier for the addition of the nucleophile.

The results of this work highlight the importance of including dynamic correlation in the calculation to get a properly balanced description of the chlorophenyl anion and the diradical. As shown in the **Supporting Information**, the energy curves obtained at the SA-CASSCF and EOM-SF-CCSD levels of theory have barriers for addition and are discontinuous.

Although accurate calculation of the energies requires dynamic correlation, the continuous transition from anion to diradical is evident in the underlying wave functions. For example, [Figure 3](#) shows a plot of

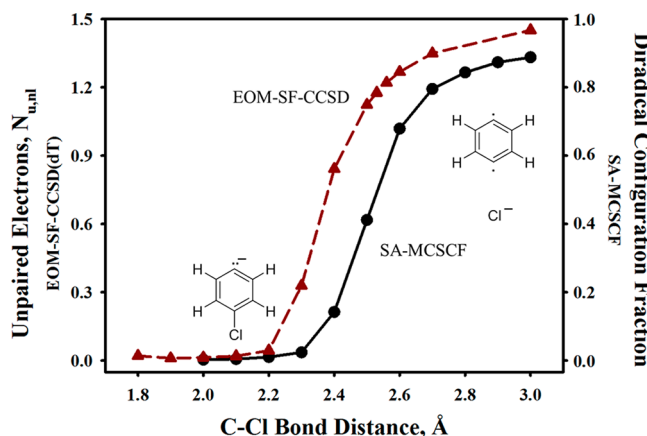


Figure 3. Extent of diradical character in the chlorophenyl anion as a function of C–Cl distance, calculated at the SA-CASSCF (black circles, right axis) and EOM-SF-CCSD (red triangles, left axis) levels of theory.

the diradical character versus C–Cl bond distance, calculated using the SA-CASSCF and EOM-SF-CCSD methods. With the SA-CASSCF, the fraction of the diradical starts near 0, as expected for the phenyl anion. Diradical character becomes appreciable as the C–Cl distance gets to 2.4–2.5 Å and approaches the asymptotic limit by 2.7–2.8 Å.⁴⁹

With the SF-CCSD calculations, the diradical character is measured by using the Head-Gordon parameter, $N_{u,\text{nl}}$, which indicates the effective number of unpaired electrons in the natural orbitals. Again, the value is close to 0 for the closed-shell anion. With this level of theory, the introduction of a diradical occurs earlier in the dissociation than it does with the SA-CASSCF calculations, starting around 2.3–2.4 Å. At

long C–Cl distance, the number of unpaired electrons is approximately 1.45, which is the value reported previously for isolated *p*-benzyne.³⁴

Another property that reflects the transition from a phenyl anion to a diradical is the geometry. Specifically, the CCC bond angle about the anionic center is relatively small (112°) in the chlorophenyl anion and then increases during the dissociation. Figure 4 shows the change in the

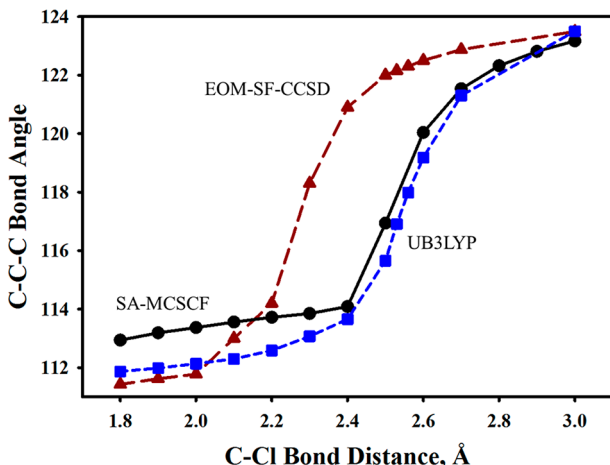


Figure 4. Optimized bond angles about the anionic carbon during the dissociation of chlorophenyl anion. Geometries optimized at the SA-CASSCF(16,14)/aug-cc-pVTZ (black circles), EOM-SF-CCSD/6-31+G* (red triangles), and UB3LYP/6-31+G* (blue squares) levels of theory.

CCC bond angle as a function of the C–Cl distance. For the EOM-SF-CCSD and UB3LYP geometries, the increase in bond angle is gradual. In the SA-CASSCF calculations, there is a slight increase in bond angle until 2.4 Å, after which the bond opens up to approach the diradical limit.

The bond angles calculated at the EOM-SF-CCSD level of theory increase earlier in the dissociation than do those calculated at the SA-CASSCF and UB3LYP levels of theory. This is consistent with the conclusions drawn from Figure 3, showing that the diradical character develops earlier in the dissociation in the CCSD calculations. In contrast, the geometries during dissociation are very similar for the SA-CASSCF and UB3LYP calculations, especially above 2.4 Å.

CONCLUSIONS

The barrierless addition of chloride nucleophile to *p*-benzyne is readily understood from a first-principles consideration of the effect of the nucleophile on the wave function of the homosymmetric diradical. As the nucleophile approaches, it polarizes the diradical, which introduces zwitterionic character into the wave function, in the manner described by Salem and Rowland.³⁰ Because the extent of polarization depends on the distance between the diradical and the nucleophile, the transition from diradical to anion during the addition occurs with a continuous change in the electronic structure. Consequently, it is not possible to establish a point at which the system transitions from diradical to closed-shell. This conclusion is similar to those obtained by Michl and co-workers,⁵⁰ who showed that perturbations that break the degeneracy of the orbitals lead to increased closed-shell character. Together, the results show that there are no restrictions, symmetry or otherwise, on the addition of a nucleophile to a homosymmetric diradicals, consistent with the first-principles analysis provided above. Correspondingly, this analysis should also apply to the addition of an electrophile, which would similarly polarize the diradical (albeit in the

opposite direction) and add with a continuous transition from diradical to closed-shell.

The description of the *p*-chlorophenyl anion as a polarized diradical is similar to the recent studies by dos Passos Gomes and Alabugin,³⁹ who have utilized the gold cation adduct as a polarized *p*-benzyne, amenable to nucleophilic addition, and by Das et al.,⁴⁰ who have examined the nucleophilic addition to unsymmetrical benzenes. This work reiterates the fact that zwitterionic character in diradical wave functions is a matter of degree,³⁰ and that it is induced in the presence of a nucleophile or electrophile.

The lack of a barrier for the addition of the chloride found in this work does rely on the fact that it is an anionic nucleophile, leading to the formation of an anionic product. As has been proposed previously for *m*-benzyne,²³ the addition of a neutral nucleophile, even if energetically favorable, could have a barrier resulting from the formation of the zwitterionic product. Similarly, the differences in the attractive potentials for the approach of other nucleophiles with different ionic radii and polarizabilities, such as bromide or iodide, could create electrostatic barriers, depending on the location and depth of the energy well. In fact, the enthalpy of formation of *p*-benzyne obtained by the dissociation of *p*-bromophenyl anion reported by Wenthold and Squires⁴¹ was measured to be 2 kcal/mol higher than that obtained from the chlorinated precursor, which could be due the presence of a barrier for the dissociation in excess of the adiabatic dissociation energy.⁴¹ However, the difference is well within the uncertainty of the measurements and therefore too small to draw any conclusions. Finally, differences in solvation of the nucleophile could also lead to energy barriers, as has been found for the addition of halides to *p*-benzyne.^{24,28} Although these electrostatic factors could affect the energies and even create barriers, the transition of the wave function during the reaction should not be affected by these factors.

Although this work provides a theoretical framework for understanding the nucleophilic addition to homosymmetric diradicals, it does not apply to *heterosymmetric* diradicals, in which the nonbonding molecular orbitals have different symmetry properties. Yet, it has been found that heterosymmetric diradicals can also undergo nucleophilic addition.^{51–53} The theoretical description of nucleophilic addition to heterosymmetric diradicals is provided in the following paper.⁵⁴

ASSOCIATED CONTENT

Supporting Information

The Supporting Information is available free of charge on the ACS Publications website at DOI: 10.1021/acs.joc.8b01413.

Geometries, energies, and wave function information obtained from SA-CASSCF and EOM-SF-CCSD(dT) calculations, including CI coefficients for the SA-CASSCF calculations and Head-Gordon parameters, $N_{u,nb}$ from EOM-SF-CCSD calculations; comparison of dissociation curves calculated with and without dynamic correlation (PDF)

AUTHOR INFORMATION

Corresponding Authors

*E-mail: pgw@purdue.edu.

*E-mail: winter@iastate.edu.

ORCID

Paul G. Wenthold: 0000-0002-8257-3907

Arthur H. Winter: 0000-0003-2421-5578

Notes

The authors declare no competing financial interest.

ACKNOWLEDGMENTS

This work was supported by the National Science Foundation (CHE15-65755 to P.G.W.; CHE17-64235 to A.H.W.). We are thankful to Profs. John Stanton and Igor Alabugin for helpful discussion and comments, and to Dr. Natalie Orms for assistance with the Head-Gordon index calculation.

REFERENCES

- (1) Dunitz, J. D. Chemical Reaction Paths. *Philos. Trans. R. Soc., B* **1975**, *272*, 99–108.
- (2) Pauling, L. *The Nature of the Chemical Bond and the Structure of Molecules and Crystals*; Cornell University Press, 1939.
- (3) Bunnett, J. F. Aromatic Substitution by the SRN1Mechanism. *Acc. Chem. Res.* **1978**, *11*, 413–20.
- (4) Rossi, R. A.; Guastavino, J. F.; Buden, M. E. Radical-Nucleophilic Aromatic Substitution. In *Arene Chemistry: Reaction Mechanisms and Methods for Aromatic Compounds*; Mortier, J., Ed.; John Wiley & Sons, Inc.: Hoboken, NJ, 2015; pp 243–268.
- (5) Rossi, R. A.; Palacios, S. M. On the SRN1-SRN2Mechanistic Possibilities. *Tetrahedron* **1993**, *49*, 4485–94.
- (6) Rossi, R. A.; Pierini, A. B.; Palacios, S. M. Nucleophilic Substitution by the SRN1 Mechanism on Alkyl Halides. *Adv. Free Radical Chem. (Greenwich, Conn.)* **1990**, *1*, 193–252.
- (7) Shaik, S. S. The Collage of SN2 Reactivity Patterns: a State Correlation Diagram Model. *Prog. Phys. Org. Chem.* **2007**, *15*, 197–337.
- (8) Andrieux, C. P.; Saveant, J. M.; Zann, D. Relationship Between Reduction Potentials and Anion Radical Cleavage Rates in Aromatic Molecules. *Nouv. J. Chim.* **1984**, *8*, 107–16.
- (9) Saveant, J. M. Single Electron Transfer and Nucleophilic Substitution. *Adv. Phys. Org. Chem.* **1990**, *26*, 1–130.
- (10) Saveant, J. M. Dynamics of Cleavage and Formation of Anion Radicals into and from Radicals and Nucleophiles. Structure-Reactivity Relationships in SRN1 Reactions. *J. Phys. Chem.* **1994**, *98*, 3716–24.
- (11) Adcock, W.; Andrieux, C. P.; Clark, C. I.; Neudeck, A.; Saveant, J.-M.; Tardy, C. Evidence for Orbital Symmetry Restrictions in Intramolecular Dissociative Electron Transfer. *J. Am. Chem. Soc.* **1995**, *117*, 8285–6.
- (12) Lorance, E. D.; Kramer, W. H.; Gould, I. R. Barrierless Electron Transfer Bond Fragmentation Reactions. *J. Am. Chem. Soc.* **2004**, *126*, 14071–8.
- (13) Evoniuk, C. J.; Gomes, G. d. P.; Hill, S. P.; Fujita, S.; Hanson, K.; Alabugin, I. V. Coupling N–H Deprotonation, C–H Activation, and Oxidation: Metal-Free C(sp³)–H Aminations with Unprotected Anilines. *J. Am. Chem. Soc.* **2017**, *139*, 16210–16221.
- (14) Rossi, R. A.; deRossi, R. H.; Lopez, A. F. A Molecular Orbital Approach to the SRN1Mechanism of Aromatic Substitution. *J. Org. Chem.* **1976**, *41*, 3367–71.
- (15) Salem, L. The Electronic Theory of Photochemical Reactions. *Isr. J. Chem.* **1975**, *14*, 89–104.
- (16) Berson, J. A. Diradicals: Conceptual, Inferential, and Direct Methods for the Study of Chemical Reactions. *Science (Washington, DC, U. S.)* **1994**, *266*, 1338–9.
- (17) Johnston, L. J.; Scaiano, J. C. Time-Resolved Studies of Biradical Reactions in Solution. *Chem. Rev.* **1989**, *89*, 521–47.
- (18) Abe, M. New Development of Reactive Intermediate Chemistry: A Case Study of Singlet Biradicals. *Yuki Gosei Kagaku Kyokaishi* **2007**, *65*, 16–22.
- (19) Abe, M. Diradicals. *Chem. Rev. (Washington, DC, U. S.)* **2013**, *113*, 7011–7088.
- (20) Pilling, M. J. Reactions of Hydrocarbon Radicals and Biradicals. *J. Phys. Chem. A* **2013**, *117*, 3697–3717.
- (21) Williams, P. E.; Jankiewicz, B. J.; Yang, L.; Kenttamaa, H. I. Properties and Reactivity of Gaseous Distonic Radical Ions with Aryl Radical Sites. *Chem. Rev. (Washington, DC, U. S.)* **2013**, *113*, 6949–6985.
- (22) Nelson, E. D.; Artau, A.; Price, J. M.; Kenttamaa, H. I. m-Benzyne Reacts as an Electrophile. *J. Am. Chem. Soc.* **2000**, *122*, 8781–8782.
- (23) Nelson, E. D.; Artau, A.; Price, J. M.; Tichy, S. E.; Jing, L.; Kenttamaa, H. I. meta-Benzyne Reacts as an Electrophile. *J. Phys. Chem. A* **2001**, *105*, 10155–10168.
- (24) Perrin, C. L.; Rodgers, B. L.; O'Connor, J. M. Nucleophilic Addition to a p-Benzyne Derived from an Enediyne: A New Mechanism for Halide Incorporation into Biomolecules. *J. Am. Chem. Soc.* **2007**, *129*, 4795–4799.
- (25) Wentholt, P. G.; Squires, R. R.; Lineberger, W. C. Ultraviolet Photoelectron Spectroscopy of the *o*-, *m*-, and *p*-Benzyne Negative Ions. Electron Affinities and Singlet-Triplet Splittings for *o*-, *m*-, and *p*-Benzyne. *J. Am. Chem. Soc.* **1998**, *120*, 5279–5290.
- (26) Amegayibor, F. S.; Nash, J. J.; Lee, A. S.; Thoen, J.; Petzold, C. J.; Kenttamaa, H. I. Chemical Properties of a para-Benzyne. *J. Am. Chem. Soc.* **2002**, *124*, 12066–12067.
- (27) Kirkpatrick, L. M.; Vinueza, N. R.; Jankiewicz, B. J.; Gallardo, V. A.; Archibald, E. F.; Nash, J. J.; Kenttamaa, H. I. Experimental and Computational Studies on the Formation of Three para-Benzynes Analogues in the Gas Phase. *Chem. - Eur. J.* **2013**, *19*, 9022–9033.
- (28) Perrin, C. L.; Reyes-Rodriguez, G. J. Reactivity of Nucleophiles Toward a p-Benzyne Derived from an Enediyne. *J. Phys. Org. Chem.* **2013**, *26*, 206–210.
- (29) Hoffmann, R.; Imamura, A.; Hehre, W. J. Benzynes, Dehydroconjugated Molecules, and the Interaction of Orbitals Separated by a Number of Intervening Sigma Bonds. *J. Am. Chem. Soc.* **1968**, *90*, 1499–1509.
- (30) Salem, L.; Rowland, C. Electronic Properties of Diradicals. *Angew. Chem., Int. Ed. Engl.* **1972**, *11*, 92–111.
- (31) Winkler, M.; Sander, W. The Structure of meta-Benzynes Revisited-A Close Look into σ -Bond Formation. *J. Phys. Chem. A* **2001**, *105*, 10422–10432.
- (32) Gao, J.; Jankiewicz, B. J.; Reece, J.; Sheng, H.; Cramer, C. J.; Nash, J. J.; Kenttamaa, H. I. On the Factors that Control the Reactivity of meta-Benzynes. *Chem. Sci.* **2014**, *5*, 2205–2215.
- (33) Nash, J. J.; Nizzi, K. E.; Adeuya, A.; Yurkovich, M. J.; Cramer, C. J.; Kenttamaa, H. I. Demonstration of Tunable Reactivity for meta-Benzynes. *J. Am. Chem. Soc.* **2005**, *127*, 5760–5761.
- (34) Orms, N.; Rehn, D. R.; Dreuw, A.; Krylov, A. I. Characterizing Bonding Patterns in Diradicals and Triradicals by Density-Based Wave Function Analysis: A Uniform Approach. *J. Chem. Theory Comput.* **2018**, *14*, 638–648.
- (35) Wierschke, S. G.; Nash, J. J.; Squires, R. R. A Multiconfigurational SCF and Correlation-Consistent CI Study of the Structures, Stabilities, and Singlet-Triplet Splittings of *o*-, *m*-, and *p*-Benzyne. *J. Am. Chem. Soc.* **1993**, *115*, 11958–67.
- (36) Peterson, P. W.; Mohamed, R. K.; Alabugin, I. V. How to Lose a Bond in Two Ways - The Diradical/Zwitterion Dichotomy in Cycloaromatization Reactions. *Eur. J. Org. Chem.* **2013**, *2013*, 2505–2527.
- (37) Logan, C. F.; Chen, P. Ab Initio Calculation of Hydrogen Abstraction Reactions of Phenyl Radical and p-Benzyne. *J. Am. Chem. Soc.* **1996**, *118*, 2113–14.
- (38) Schottelius, M. J.; Chen, P. 9,10-Dehydroanthracene: p-Benzyne-Type Biradicals Abstract Hydrogen Unusually Slowly. *J. Am. Chem. Soc.* **1996**, *118*, 4896–903.
- (39) dos Passos Gomes, G.; Alabugin, I. V. Drawing Catalytic Power from Charge Separation: Stereoelectronic and Zwitterionic Assistance in the Au(I)-Catalyzed Bergman Cyclization. *J. Am. Chem. Soc.* **2017**, *139*, 3406–3416.
- (40) Das, E.; Basak, S.; Anoop, A.; Basak, A. An Experiment cum Computational Study on the Regioselectivity of Nucleophilic Addition to Unsymmetrical p-Benzynes Derived from Bergman Cyclization of Enediynes. *J. Org. Chem.* **2018**, *83*, 7730–7740.
- (41) Wentholt, P. G.; Squires, R. R. Biradical Thermochemistry from Collision-Induced Dissociation Threshold Energy Measurements.

Absolute Heats of Formation of ortho-, meta-, and para-Benzyne. *J. Am. Chem. Soc.* **1994**, *116*, 6401–12.

(42) Wentholt, P. G.; Wierschke, S. G.; Nash, J. J.; Squires, R. R. $\alpha,3$ -Dehydrotoluene: Experimental and Theoretical Evidence for a Singlet Ground State. *J. Am. Chem. Soc.* **1993**, *115*, 12611–12.

(43) Wentholt, P. G.; Wierschke, S. G.; Nash, J. J.; Squires, R. R. Experimental and Theoretical Studies of the Mechanism and Thermochemistry of Formation of α,n -Dehydrotoluene Biradicals from Gas-Phase Halide Elimination Reactions. *J. Am. Chem. Soc.* **1994**, *116*, 7378–92.

(44) There are additional contributions to the molecular orbitals besides ϕ_1 and ϕ_2 , but they are not critical for the analysis.

(45) Aquilante, F.; Autschbach, J.; Carlson, R. K.; Chibotaru, L. F.; Delcey, M. G.; De Vico, L.; Fdez. Galván, I.; Ferré, N.; et al. MOLCAS 8: New Capabilities for Multiconfigurational Quantum Chemical Calculations across the Periodic Table. *J. Comput. Chem.* **2016**, *37*, 506–541.

(46) Finley, J.; Malmqvist, P.-A.; Roos, B. O.; Serrano-Andres, L. The Multi-State CASPT2 Method. *Chem. Phys. Lett.* **1998**, *288*, 299–306.

(47) Head-Gordon, M. Characterizing unpaired electrons from the one-particle density matrix. *Chem. Phys. Lett.* **2003**, *372*, 508–511.

(48) Plasser, F.; Wormit, M.; Dreuw, A. New tools for the systematic analysis and visualization of electronic excitations. I. Formalism. *J. Chem. Phys.* **2014**, *141*, 024106.

(49) As indicated above, the MS-CASPT2 approach should give a better description of the multiconfigurational wave function. We have calculated the diradical configuration fractions at the MS-CASPT2/aug-cc-pVDZ level of theory, and they are about 20% lower than those obtained with the SA-CASSCF methods. However, the relative values as a function of distance are essentially the same. See [Supporting Information](#) for additional details.

(50) Bonačić-Koutecký, V.; Koutecký, J.; Michl, J. Neutral and Charged Biradicals, Zwitterions, Funnels in S1, and Proton Translocation: Their Role in Photochemistry, Photophysics, and Vision. *Angew. Chem., Int. Ed. Engl.* **1987**, *26*, 170–189.

(51) Myers, A. G.; Dragovich, P. S.; Kuo, E. Y. Studies on the Thermal Generation and Reactivity of a Class of (σ,π) -1,4-Biradicals. *J. Am. Chem. Soc.* **1992**, *114*, 9369–86.

(52) Myers, A. G.; Kuo, E. Y.; Finney, N. S. Thermal Generation of $\alpha,3$ -Dehydrotoluene from (Z)-1,2,4-Heptatrien-6-yne. *J. Am. Chem. Soc.* **1989**, *111*, 8057–9.

(53) Du, L.; Qiu, Y.; Lan, X.; Zhu, R.; Phillips, D. L.; Li, M.-D.; Dutton, A. S.; Winter, A. H. Direct Detection of the Open-Shell Singlet Phenyloxenium Ion: An Atom-Centered Diradical Reacts as an Electrophile. *J. Am. Chem. Soc.* **2017**, *139*, 15054–15059.

(54) Wentholt, P. G.; Winter, A. H. Nucleophilic Addition to Singlet, Heterosymmetric Diradicals. *J. Org. Chem.* **2018**, DOI: [10.1021/acs.joc.8b01414](https://doi.org/10.1021/acs.joc.8b01414).